Vorinostat with Sustained Exposure and High Solubility in Poly(ethylene glycol)-b-poly(DL-lactic acid) Micelle Nanocarriers: Characterization and Effects on Pharmacokinetics in Rat Serum and Urine

Elham A. Mohamed[a,b], **Yunqi Zhao**[c], **Mahasen M. Meshali**[b], **Connie M. Remsberg**[a], **Thanaa M. Borg**[b], **Abdel Monem M. Foda**[b], **Jody K. Takemoto**[a], **Casey Sayre**[d], **Stephanie Martinez**[d], **Neal M. Davies**[d], and **M. Laird Forrest**[c,*]

[a]College of Pharmacy, Department of Pharmaceutical Sciences, Washington State University, Pullman, WA 99164-6534, USA

[b]Department of Pharmaceutics, Faculty of Pharmacy, Mansoura University, Mansoura, Egypt

[c]Department of Pharmaceutical Chemistry, The University of Kansas, Simons Labs, 2095 Constant Ave, Rm. 136B, Lawrence, Kansas 66047-3729, USA

[d]Faculty of Pharmacy, University of Manitoba, Winnipeg, MB R3T 2N2, Canada

Abstract

The histone deacetylase inhibitor suberoylanilide hydroxamic acid, known as vorinostat, is a promising anti-cancer drug with a unique mode of action; however, it is plagued by low water solubility, low permeability, and suboptimal pharmacokinetics. In this study, poly(ethylene glycol)-b-poly(DL-lactic acid) (PEG-b-PLA) micelles of vorinostat were developed. Vorinostat's pharmacokinetics in rats were investigated after intravenous (i.v.) (10 mg/kg) and oral (50 mg/kg) micellar administrations and compared to a conventional PEG400 solution and methylcellulose suspension. The micelles increased the aqueous solubility of vorinostat from 0.2 mg/ml to 8.15 ± 0.60 mg/ml and 10.24 ± 0.92 mg/ml at drug to nanocarrier ratios of 1:10 and 1:15, respectively. Micelles had nanoscopic mean diameters of 75.67 ± 7.57 nm and 87.33 ± 8.62 nm for 1:10 and 1:15 micelles, respectively, with drug loading capacities of $9.93 \pm 0.21\%$ and 6.91 ± 1.19 %, and encapsulation efficiencies of $42.74 \pm 1.67\%$ and $73.29 \pm 4.78\%$, respectively. The micelles provided sustained exposure and improved pharmacokinetics characterized by a significant increase in serum half-life, area under curve, and mean residence time. The micelles reduced vorinostat clearance particularly after i.v. dosing. Thus, PEG-b-PLA micelles significantly improved the oral and intravenous pharmacokinetics and bioavailability of vorinostat, which warrants further investigation.

Keywords

*Correspondence to: Dr. Laird Forrest, University of Kansas, 2095 Constant Ave, Lawrence, KS 66047. mforrest@ku.edu.

Introduction

Block copolymers spontaneously form nanoscopic micelles in water, and they are efficient solubilizing agents for poorly water soluble drugs. Such ability originates from a hydrophobic core that serves as a reservoir of the drug molecules incorporated by chemical, physical or electrostatic interactions.[1] The core is sterically stabilized by a hydrophilic corona, and the resulting micelles are kinetically stable when diluted below the critical micelle concentration because of chain entanglement and slow unimer exchange. Beyond solubilization, block copolymer micelles can retain the drug leading to prolonged *in vivo* circulation times. The nanocarriers are sufficiently large to avoid renal excretion, yet small enough to bypass filtration by interendothelial cell slits in the spleen.[2] In addition, they have the potential for passive drug targeting to solid tumors via the enhanced permeability and retention (EPR) effect.[3]

Histone deacetylase (HDAC) is an enzyme that removes acetyl groups from lysine residues of proteins, including histones and transcription factors.[4] Certain cancers overexpress HDACs resulting in over-compaction of the histone-DNA complex and repression of gene transcription for an array of genes including those for cell-cycle control, apoptosis, and tumor suppression.[5] The HDAC inhibitor, suberoylanilide hydroxamic acid (SAHA, vorinostat, Fig. 1A), is used in the treatment of cutaneous T-cell lymphoma (CTCL).[6,7] Vorinostat is marketed by Merck & Co., Inc. as an oral capsule under the brand name Zolinza®.[5] Although the therapeutic potential of vorinostat is great [8,9,10], vorinostat is plagued by poor aqueous solubility (0.2 mg/ml) and low permeability (a log partition coefficient of 1.9) as indicated by its Class IV designation in Biopharmaceutics Classification System (BCS). [11] Because of this, development of a parenteral formulation of vorinostat has been hindered. For instance, in early clinical studies, the intravenous (i.v.) formulations of vorinostat were dissolved in sodium hydroxide, adjusted to pH 11.2, and administered over a two hour infusion.[12] Other attempts to develop a parenteral formulation of vorinostat are limited but include a cyclodextrin formulation.[11]

Vorinostat is also plagued by suboptimal pharmacokinetics including low bioavailability (43% for humans and 11% for rats), extensive serum clearance, and a short elimination half-life of approximately 2 hours in both animal and human studies. [5,13,14,4,15] Much of the short half-life and limited overall exposure of vorinostat is related to its rapid metabolism, which is its predominate route of elimination.[13] Vorinostat is metabolized via two metabolic pathways including glucuronidation and hydrolysis followed by β-oxidation. These pathways produce two inactive metabolites, a vorinostat glucuronide and a vorinostat hydrolysis metabolite, 4-anilino-4-oxobutanoic acid, both of which are excreted in the urine.[16] Therefore, it is of medical importance to develop novel formulations of vorinostat for both oral and parenteral administrations that improve solubility and the overall disposition profile of vorinostat.

Among the commonly used copolymers, poly(ethylene glycol)-b-poly(lactic acid) (PEG-b-PLA, Fig. 1B) has been selected to develop micellar formulations of vorinostat because it's polymer backbone is based on biodegradable and biocompatible poly(lactide) (PLA) and poly(ethylene glycol) (PEG), and PEG-b-PLA is reported to increase the drug aqueous

solubility, reduce the burst effect, and prolong the *in vivo* residence time of drugs due to steric stabilization against opsonization and subsequent phagocytocis.[17,18,19,20] As well, degradation products of PEG–PLA block copolymer can enter the tricarboxylic acid cycle or be eliminated by the kidney.[21] In addition, the reversal of multiple drug resistance by PEG-b-PLA micelles was proven as a major reason of the relevance of paclitaxel uptake by tumor cells *in vitro*.[22] Consequently, PEG-b-PLA is being widely investigated as a nanocarrier of different sparingly soluble drugs including anticancer agents. Moreover, PEG-b-PLA micelles have entered phase III clinical trials as a substitute for toxic Cremophor® EL in the delivery of paclitaxel in cancer therapy. [23,24]

Therefore, it was warranted to develop, characterize, and optimize novel nanoformulations of vorinostat using the PEG–b-PLA nanocarrier. In this study, the pharmacokinetics of vorinostat in rat serum and urine were investigated following i.v. and oral administrations and compared to the respective controls of PEG400 solution and 2% methylcellulose suspension.

Experimental

Chemicals and reagents

Vorinostat and daidzein were purchased from LC laboratories (Woburn, MA, USA). Poly(ethylene glycol)-b-poly(DL-lactic acid) (PEG–b-PLA) block copolymer of PEG/PLA ratio of 5000/2000 was purchased from Polymer Source Inc. (Dorval, Quebec, Canada). HPLC-grade acetonitrile and water were purchased from J.T. Baker (Philipsburg, NJ, USA). Other chemicals were of analytical grade. Healthy male Sprague-Dawley rats with an average body weight of ca. 280 g were obtained from Simonsen Labs (Gilroy, CA, USA).

Preparation of vorinostat loaded PEG-b-PLA micelles

Vorinostat loaded PEG-b-PLA micelles were prepared at drug to copolymer ratios of 1:10 and 1:15. Both vorinostat and PEG-b-PLA were dissolved in a minimum volume of tetrahydrofuran and acetone mixture in a ratio of 4:1, respectively, and added drop-wise at a rate of 50 μL/min to vigorously stirred ddH$_2$O. Organic solvents then were removed by stirring under a nitrogen purge overnight. After removing the organic solvents, PEG-b-PLA micelles were passed through a 0.22-μm polyethersulfone filter to remove insoluble material and unincorporated drug.[25] Micellar solutions were further concentrated by rotary evaporation to obtain vorinostat concentrations > 8 mg/ml, which was suitable for dosing volumes of   0.5 ml intravenously (10 mg/kg) and   2 ml orally (50 mg/kg) using rats with an average weight of 280 g.

Characterization of vorinostat loaded PEG-b-PLA micelles

The formation of PEG-b-PLA micelles was determined by size exclusion chromatography (SEC) using a Shimadzu 2010CHT system with 0.8 ml/min ddH$_2$O as the mobile phase on a Shodex OHpak-806 HQ column (Showa Denko America, NY) thermostated at 40°C. Peaks were detected using an evaporative light scattering detector (ELSD-LTII, Shimadzu, Lenexa, KS). Narrow molecular weight distribution polyethylene glycols (Scientific Polymer Products, Ontario, NY) were used as standards for SEC analysis. To confirm the

drug was encapsulated in the micelles, SEC peak fractions were collected and dried by Speed-Vap. The dried micelle fractions were redissolved in acetonitrile and then analyzed by reversed-phase HPLC. The system was identical to the above but with UV detection (254 nm) and 0.8-mL/min acetonitrile:methanol:water:trifluoroacetic acid (32:32:36:0.1) mobile phase on an ODS-100 C_{18} 5-μm x 150-mm column (Tosoh, Tessenderlo, Belgium) thermostated to 40°C.

Measurements of micelle size were performed using Dynamic Light Scattering (DLS) with a Malvern Nano ZS instrument and DTS software (Malvern Instruments Ltd, Malvern, Worcestershire, UK). The loading efficiency (LE) and entrapment efficiency (EE) of vorinostat in PEG-b-PLA micelles were calculated according to the following equations:[26]

$$LE\% = \frac{\text{Weight of the drug in the micelles}}{\text{Weight of the micelles}} \times 100\%$$

$$EE\% = \frac{\text{Weight of the drug in the micelles}}{\text{Weight of the feeding drug}} \times 100\%$$

Vorinostat concentration in the prepared micelles was determined with a method previously validated at our laboratory that is described below.[27] The micelles solution was diluted to a range within our calibration curve before addition of the internal standard. The vorinostat-PEG-b-PLA micelles used for characterization were prepared as detailed above. The loading efficiency (LE) was calculated according to the above equation using micelles dried to constant weight.

The *in vitro* stability of the micelles was determined over a period of 5 days, the same period of the pharmacokinetic study, by measuring the micelle size daily by DLS and measuring drug incorporation after filtration using the validated LC/MS method.

Surgical procedures

Male Sprague-Dawley rats (ca. 280 g) from Simonsen Labs (Gilroy, CA, USA) were acclimated for a minimum of 3 days in temperature-controlled rooms with a 12 h light/dark cycle and given food (Purina Rat Chow 5001) and water *ad libitum*. The day before the pharmacokinetic experiment, the right jugular veins of the rats were catheterized with sterile silastic cannula (Dow Corning, Midland, MI, USA) under isoflurane anesthesia via procedures previously published.[28] This involved exposure of the vessel prior to cannula insertion. After cannulation, Intramedic PE-50 polyethylene tubing (Becton, Dickinson and Company, Franklin Lakes, NJ, USA) connected to the cannula was exteriorized through the dorsal skin. The cannula was flushed with 0.9% saline. The animals were transferred to metabolic cages and fasted overnight. Animal use protocols were approved by The Institutional Animal Care and Use Committee at Washington State University, in accordance with "The Guide for Care and Use of Laboratory Animals" (National Academy Press, revised 1996).

Pharmacokinetic Study

On the days of the experiment, the animals were dosed intravenously (10 mg/kg) via cannula with vorinostat in polyethylene glycol 400 (PEG400) as a control or vorinostat micelles using PEG-b-PLA at two different drug to nanocarrier ratios (1:10 and 1:15) (n = 5 for each treatment group). The rats were given 0.5 ml of each formulation as an i.v. bolus via cannula. PEG 400 was given intravenously in 0.5 ml of dosing solution. Aqueous solution of micelles was dosed intravenously in volume ranged from 0.2 to 0.4 ml. The cannula was flushed with normal saline after each IV dose administration. For oral treatment, the rats were administered vorinostat (50 mg/kg) as a suspension in 2% methylcellulose as control or as a micelle solution via oral gavage (n = 5 for each treatment group). The rats were given 2 ml of each formulation orally as a single dose. Vorinostat as 2% MC suspension was given orally in 0.5 to 1 ml. For orally dosed micelles solution ranging from 1.04 to 1.93 ml was used.

After dosing, serial blood samples (ca. 0.30 ml) were collected from the cannula at 0, 1, 15 and 30 min, then 1, 2, 4, 6, 12, 24, 48, 72, 96, and 120 h after i.v. administration, or at 0, 15 and 30 min, then 1, 2, 4, 6, 12, 24, 48, 72, 96, and 120 h after oral administration, and then the cannula was flushed with 0.9% saline. After dosing and after each serial blood sampling, blinded observers were present to record any visible behavior, bleeding, or change in overall appearance of the animal as signs of acute toxicity. Each blood sample was collected into regular polypropylene microcentrifuge tubes and following centrifugation; the serum was collected and stored at –20°C until analyzed. Urine samples were collected overnight (0 hr sample) and over the time intervals of 0–2, 2–6, 6–12, 12–24, 24–48, 48–72, 72–96 and 96–120 h following both i.v. and oral administration and were stored at – 20°C until analyzed.

LC/MS quantitative assay of vorinostat

Vorinostat concentrations in the prepared micelle solution and collected serum and urine samples were determined using a reversed-phase HPLC method with ESI-mode mass spectrometry detection that was previously validated by our laboratory. A Shimadzu LCMS-2010 EV liquid chromatograph mass spectrometer system (Kyoto, Japan) connected to the HPLC portion consisting of two LC-10AD pumps, a SIL-10AD VP auto injector, a SPD-10A VP UV detector, and a SCL-10A VP system controller was used. Data analysis was accomplished using Shimadzu LCMS Solutions Version 3 software. The mass spectrometer conditions consisted of a curved desolvation line (CDL) temperature of 200°C and a block temperature of 200°C, a detector voltage of 1.5 kV, and nitrogen nebulizing gas at 1.5 L/min. The analytical column used was a Phenomenex Luna C_{18} (2) (250 × 4.60 mm, i.d. 5 μm). The mobile phase consisted of acetonitrile, water, and formic acid (30:70:0.1, v/v/v), and it was filtered (0.2 μm) and degassed under reduced pressure prior to use. Separation was carried out isocratically at a flow rate of 0.6 ml/min. To the micelles solution, serum or urine (100 μl), and 50 μl of internal standard solution, daidzein (100 μg/ ml), was added. The mixture was vortexed for 30 s (Vortex Genie-2, VWR Scientific, West Chester, PA, USA). To serum samples, 1 ml of cold acetonitrile (–20°C) was added to precipitate serum proteins. Urine samples were extracted with 0.5 ml of methanol. Samples were then vortexed for 30 s and centrifuged at 10,000 rpm for 5 min (Beckman Microfuge centrifuge, Beckman Coulter Inc., Fullerton, CA, USA). The serum supernatant and all other

samples were then evaporated to dryness by a stream of nitrogen gas. The residue was reconstituted with 100 μl of mobile phase, vortexed for 30 s, recentrifuged, supernatant transferred to HPLC vials, and 10 μl was injected into the LC/MS system. Quantification was based on calibration curves obtained using vorinostat with an internal standard, and the data were fitted using unweighted least squares linear regression. Vorinostat and the internal standard, daidzein were monitored in selected ion monitoring (SIM) positive mode at *m/z* 265 and 255, respectively. In addition, the assay allowed monitoring of both a glucuronidated metabolite (vorinostat-O-glucuronide) and a hydrolysis metabolite (4-anilino-4-oxobutanoic acid) via the SIM positive mode at *m/z* 441 and 194, respectively. The metabolites were monitored assuming equal ionization of the metabolites with vorinostat. Metabolite concentrations in serum and urine were estimated using the standard curve of vorinostat in the respective matrix.

Pharmacokinetic analysis

Pharmacokinetic analysis was completed using data from individual rats for which the mean and standard error of the mean (SEM) were calculated for each group except for T_{max} which was represented as median and range. Pharmacokinetic parameters were estimated using WinNonlin® (version 1.0) using noncompartmental analysis. The half-life of the terminal elimination phase ($t_{1/2}$) was calculated using the following equation: $t_{1/2} = 0.693/K_E$. The area under the concentration time curve ($AUC_{0-Clast}$) was calculated using the linear/logarithmic trapezoidal method. Summation of $AUC_{0-Clast}$ and the concentration at the last measured point divided by K_E yielded $AUC_{0-\infty}$ ($AUC_{0-Clast} + Clast/K_E$). Mean residence time (MRT) was calculated by dividing $AUMC_{0-\infty}$ (area under the first moment curve) by $AUC_{0-\infty}$. Clearance (CL) was estimated using the equation of CL= $D/AUC_{0-\infty}$, where D is the dose. Volume of distribution (Vss) was calculated as CL x MRT_{last} for IV formulations. For oral formulations, Vss/F was calculated as $Dose_{po}/AUC_{po}$ x MRT_{IV}. The fraction excreted in urine unchanged (F_e) was calculated by dividing the total cumulative amount of vorinostat excreted in urine (Xu) by the dose, renal clearance (CL_{renal}) by multiplying F_e by CL, and non-renal clearance (CL_{NR}) by subtracting CL_{renal} from CL. The C_{max} and corresponding T_{max} were obtained directly from the observed data. Absolute oral bioavailability (*F*) was calculated from serum data in comparison to i.v. PEG4000 data using the relationship *F* (%) = [(dose$_{iv}$ × $AUC_{0-\infty, oral}$)/ (dose$_{oral}$ × $AUC_{0-\infty, iv}$)] × 100.

Statistical analysis

Micelle characterization data were represented as mean and standard deviation (mean ± SD) of triplicate determinations. Pharmacokinetic parameters were reported as mean and standard error of the mean (mean ± SEM) of replicate determinations, n = 5. Pharmacokinetic results were statistically analyzed based on one-way analysis of variance (ANOVA) test followed by Tukey-Kramer test to compare between pairs. This statistical analysis was computed using GraphPad InStat version 3.0 (GraphPad Software, Inc., San Diego, CA, USA).

Results and discussion

Micelle characterization

Micelles appeared as a distinct peak on SEC, with a retention time of 7.7 min for the PEG-b-PLA micelles (7,050 Da using PEG standards) and 12.1 min for the free polymer (unimers) (Fig. 1). The micelle fractions were collected and assayed for drug content by HPLC with UV detection. Vorinostat was found in the micelle SEC peak (5.5 to 7.5 mL) but not the unimer peak, and the HPLC retention time (4.92 min) was identical to the standard with no additional peaks.

Formulation of vorinostat with PEG-b-PLA increased the aqueous solubility from 0.2 mg/ml[11] to 8.15 ± 0.60 mg/ml (41-fold) and 10.24 ± 0.92 mg/ml (51-fold) at drug to nanocarrier ratios of 1:10 and 1:15, respectively. Mean diameters as determined by DLS were 75.67 ± 7.57 nm for 1:10 micelles and 87.33 ± 8.62 nm for 1:15 micelles. The loading efficiency (LE) for 1:10 and 1:15 micelles were $9.93 \pm 0.21\%$ and $6.91 \pm 1.19\%$, respectively. The entrapment efficiency (EE) of vorinostat-loaded micelles at a drug to carrier ratio of 1:15 ($73.29 \pm 4.78\%$) was higher than that of micelles prepared using 1:10 drug to carrier ratio ($42.74 \pm 1.67\%$). In agreement, it has been reported that with the increase in feeding paclitaxel in PEG-PLA micelles from 10% to 50%, encapsulation efficiency decreased from 98% to 63%.[29]

Micelle solutions at both drug to carrier ratios, 1:10 and 1:15, were stable in size and drug loading for 5 successive days after preparation when stored at 4°C. The average diameters for determinations over the five days were 82.20 ± 10.64 nm and 90.40 ± 8.91 nm versus 81 nm and 89 nm within 2 h after preparation for 1:10 and 1:15 micelles, respectively. The average concentration for determinations over the five days was 7.92 ± 0.53 mg/ml and 10.03 ± 0.71 mg/ml versus 8.15 mg/ml and 10.24 mg/ml within 2 h after preparation for 1:10 and 1:15 micelles, respectively. The micelle solutions were prepared the day prior to the pharmacokinetic study after reexamination of the micelle size and vorinostat concentration. The high stability of these micelles may be attributed to the large PEG/PLA fraction (5000/2000); it has been reported that the greater the molecular chain length in PEG-b-PLA nanoparticles, the more stable the structure will be.[21] We attempted to formulate vorinostat with micelles of 5000/6700 PEG/PLA using the same methods, but the micelles were unstable. A white sediment formed within an hour with a subsequent decrease in vorinostat concentration in the filtered supernatant. As will be discussed below, the PEG-b-PLA micelles showed significant *in vivo* stability indicated by prolonged exposure of vorinostat to the systemic circulation over this period.

Pharmacokinetics of polymeric micellar vorinostat in rat serum

Blinded observers did not report any adverse effects of the tested formulations over the length of the experiments.

Both i.v. PEG-b-PLA micelle formulations substantially altered the serum pharmacokinetics compared to PEG400 (control) (Fig. 2, Table 1). Vorinostat in PEG400 solution was rapidly eliminated to concentrations below detection limits after 2 h post-dosing (Fig. 2A and B). In accordance, the vorinostat control formulation demonstrated a short half-life ($t_{1/2} = 0.61 \pm$

0.15 h), low area under curve ($AUC_{0-\infty}$ = 2.48 ± 0.98 μg.h/ml) and a rapid serum clearance (CL = 7.64 ± 2.54 l/h/kg) (Table 1). The high volume of distribution at steady state (Vss = 2.19 ± 0.84 l/kg) exceeded the total body water (0.6 l/kg) of a rat indicating that the drug was extensively distributed. Similar results have been reported for vorinostat following i.v. administration to rats at a dose of 2 mg/kg.[13] Extensive distribution of vorinostat in control formulation may be explained in part by its high tissue uptake due to its high lipid solubility. Another HDAC inhibitor, kenedine 91, has extensive distribution that was attributed to its high lipid solubility.[30] High distribution of vorinostat to the liver as has been reported in other studies,[13] which may also account for the extensive distribution of the drug.

The micelle encapsulated vorinostat showed a sustained retention *in vivo* of up to 48 h for 1:10 micelles and 120 h for 1:15 micelles (Fig. 2A) after i.v. administration. Micellar formulations of 1:10 and 1:15 PEG-b-PLA increased vorinostat's $t_{1/2}$ to 54.46 ± 18.45 h and 112.02 ± 19.52 h, respectively (Table 1). Compared to vorinostat in PEG400, the micelle carrier increased the $AUC_{0-\infty}$ values in serum by 2.7-fold for 1:10 micelles and 15.7-fold for those prepared at 1:15 ratio of drug to nanocarrier. The CL of vorinostat decreased by 4.6-fold and 28.9-fold for 1:10 and 1:15 micelle formulations, respectively, compared to vorinostat in PEG400. Both renal (CL_{renal}) and non-renal (CL_{NR}) clearances were greatly reduced by encapsulation in micelles. This implies that these micelles hindered hepatic biotransformation and glomerular filtration of vorinostat. The reduction in CL_{renal} of vorinostat by 1:15 micelles was much higher than that seen with the 1:10 formulation. It has been reported that increases in polymer size (molecular weight or hydrodynamic volume) can lead to increases in blood circulation half-life and decreased renal clearance.[31,32] This relationship is generally non-linear and the change in blood circulation half-life and renal clearance with respect to polymer size can be dramatic.[31] This holds true when comparing polymers above the renal filtration cut off.[31,33]

The micelle formulations increased the mean residence time (MRT) of vorinostat by 107-fold and 232-fold and Vss by 7.42- and 4.47-fold at drug to carrier ratios of 1:10 and 1:15, respectively (Table 1).Inhibition of P-glycoprotein (Pgp) at the cell membrane by PEG-b-PLA polymeric micelles and subsequent release of core-encapsulated drug into the cell membrane to be internalized into the cell via endocytosis may explain the higher values of Vss compared to the control formulations.[22] Vorinostat loaded PEG-b-PLA micelles given orally showed significantly altered pharmacokinetic parameters from those of the 2% MC control formulation (Table 2, Fig. 2C and D). Both types of micelles substantially lengthened the MRT of vorinostat from 5.35 h in MC, to 128.79 and 132.76 h for the 1:10 and 1:15 formulations, respectively. Compared to vorinostat suspension, the block copolymer significantly increased the $AUC_{0-\infty}$ values of vorinostat in serum by 7.76- and 19.65-fold for 1:10 and 1:15 micelles, respectively. The serum $t_{1/2}$ of vorinostat in 1:10 and 1:15 polymeric micelles (70.86 ± 7.11 h and 79.98 ± 13.73 h, respectively) was significantly longer than that of vorinostat in 2% MC suspension (3.45 ± 0.84 h). A decrease in total clearance (Cl/*F*) vorinostat by 6.97-fold for 1:10 micelles and 18.77-fold for those with 1:15 drug to nanocarrier loading was observed, when compared to 2% MC suspension (Table 2). The volume of distribution (Vss/*F*) of vorinostat in micellar formulations given orally was increased by 5.43- and 7.32-fold for 1:10 and 1:15 micelles, respectively. These changes in

clearance and volume of distribution seen with micelles given orally maybe attributed to modification in bioavailability of vorinostat.

Following oral administration of the control and nanocarrier formulations, rapid absorption of vorinostat was evident with no statistically significant differences in time to concentration maximum (T_{max}) between the formulations seen (Table 2). The orally administered 1:15 micelles significantly increased the concentration maximum ($C_{max} = 0.453 \pm 0.087$ μg/ml) by 2.29-fold compared to the 2% MC suspension. No significant change in the C_{max} of the 1:10 micelles was noted compared to the control formulation. The absolute oral bioavailability (*F*) of the control formulation was low ($6.41 \pm 0.53\%$). Previous pharmacokinetic studies also reported a short T_{max} (0.3 ± 0.1 h) and low oral bioavailability (11%) of vorinostat following oral (10 mg/kg) dosing of rats.[13] In another study, a short T_{max} (0.17 ± 0.0 h) and low oral bioavailability (6.9%) of vorinostat following oral administration of (5 mg/kg) to Wistar rats were also documented.[14] Micellar systems at drug to carrier ratios used, 1:10 and 1:15, significantly increased *F* by 9.16- and 15.40-fold, respectively (Table 2).

The serum disposition and pharmacokinetic parameters obtained following i.v. and oral administration of control and nanocarrier formulations reveals that the micellar systems provide improved delivery and more sustained exposure. These effects were more pronounced with 1:15 micelles probably due to the higher of PEG-b-PLA micelles on decrease of drug loading as has been reported in other studies.[34] In previous reports, PEG-PLA was reported as a potential delivery system to achieve sustained release and accumulation in tumors of some poorly soluble anticancer drugs. For example, paclitaxel-loaded PEG-b-PLA micelles showed more sustained release *in vitro* and increased cellular accumulation of paclitaxel in paclitaxel-resistant human ovarian cell line A2780/T compared with free paclitaxel due to a proven inhibition of Pgp function by PEG-b-PLA micelles.[22]

Following i.v. and oral administrations, only the hydrolysis metabolite of vorinostat (4-anilino-4-oxobutanoic acid) could be detected in rat serum for up to 12 h (Fig. 3). Both 1:10 and 1:15 PEG-b-PLA micelles decreased the levels of this metabolite in serum compared to the controls, which suggests PEG-b-PLA micelles as a protectant of the drug against the hepatic metabolism.

Pharmacokinetics of polymeric micellar vorinostat in rat urine

Following i.v. administration, the total amount excreted in urine plot (Fig. 4A) demonstrates that small amounts of vorinostat are excreted in the urine with both the control and micelle formulations. The fraction excreted unchanged (F_e) of vorinostat from PEG400 (7.17 ± 0.96 %) was reduced by 2.26- and 8.63-fold by the micellar systems at 1:10 and 1:15 drug to nanocarrier ratios, respectively (Table 1). In addition, CL_{renal} of vorinostat was decreased by 10.68- and 246.91-fold following i.v. administration of the 1:10 and 1:15 micelles (Table 1). These micelles may prevent filtration in the glomeruli, as micelles are larger than the glomeruli filtration limit.

The rate elimination plots (Fig. 4B) indicate similar urinary excretion rates of vorinostat from PEG400, 1:10 and 1:15 micelles. In accordance, the amount remaining to be excreted

(ARE) plots (Fig. 4C) show that vorinostat was excreted at similar rates and most of the renally eliminated vorinostat was excreted by 72 h, 24 h and 6 h post-dosing with vorinostat in PEG400 as control, 1:10 and 1:15 micelles, respectively.

Following oral administration, the total amount excreted in urine plot (Fig. 5A) indicates that vorinostat from 2% MC suspension was excreted in higher amounts compared to the micellar systems. The majority of the renally eliminated vorinostat was excreted by 12 h in case of the control and 1:10 micelles, and by 6 h for the 1:15 micelles. The fraction excreted unchanged (F_e) of vorinostat from 2% MC suspension (0.53 ± 0.04 %) was lowered by 1.73- and 29.33-fold by the 1:10 and 1:15 micelles, respectively (Table 2). The 1:10 and 1:15 micelles given orally decreased the renal clearance (CL_{renal}/F) of vorinostat by 11.67- and 541.38-fold compared to the control (Table 2). The observed changes in CL_{renal}/F following the oral administration of micellar formulations likely can be attributed to differences in vorinostat bioavailability. A possibility of absorption of intact micelles through energy dependent internalization[35,36] or other polymeric degradation component-drug conjugates[37] in the gut has been demonstrated. These components remain too large to be filtered by the kidney and exhibit modified drug release via drug cleavage.[38] Similar polymeric conjugates of vorinostat might have hindered glomerular filtration.

Following i.v. and oral administrations, ARE is maximum for the control formulation in spite of the higher excretion rate compared to micelle formulations. This is probably due to the larger amount of vorinostat originally available to be excreted unchanged in the urine. Hence, excretion occurred over a longer period of time and vorinostat was detected in the urine until later times than observed with micelles, which appear to hinder filtration in glomeruli as indicated by lower CL_{renal} and F_e in comparison with control formulations.

Control formulations demonstrated shorter MRTs than that noticed for micelles after i.v. (0.66 ± 0.20 h) and oral (5.35 ± 1.25 h) administrations (Tables 1 and 2, respectively). However, vorinostat was excreted in the urine even at later time points. A very small amount of vorinostat in comparison to the dose was excreted unchanged in the urine as indicated by values of F_e for control formulations after i.v. (7.17 ± 0.96%) and oral (6.41 ± 0.53 %) dosing (Tables 1 and 2, respectively). In addition, the majority of renally eliminated vorinostat was excreted unchanged in the urine early within 2 h after i.v. dosing (Fig. 4A) and 6 h following oral administration (Fig. 5A).

Both hydrolysis and glucuronidated metabolites were detected in urine. Distinctly lower urinary excretion of vorinostat hydrolysis and glucuronide metabolites were excreted in urine after i.v. administration (Fig. 6A and B, respectively) than that observed following orally administered formulations (Fig. 6C and D, respectively). These results can be explained by the predominant first pass metabolism of vorinostat after oral dosing.[13] A decrease in metabolite excretion in urine following i.v. and oral administration of micellar formulations was observed (Fig. 6) possibly due to a protection by micellar system against enzymes in the liver responsible for vorinostat metabolism.

Recent reports using a rat renal proximal tubular cell line suggest possible renal toxicity of vorinostat, through protein acetylation and a decrease of antiapoptotic proteins.[39,39] Despite

the low percentage of the drug being excreted unchanged in urine as reported in this study and other studies,[13] some signs of renal toxicity including increased blood creatinine and proteinuria have been reported in some clinical studies of vorinostat.[40,41] In another study, the maximum tolerated dose of vorinostat decreased progressively as hepatic dysfunction worsened, which was associated with possible toxicity due to vorinostat metabolites.[42] The reduction in renal elimination of vorinostat in the micellar formulations may reduce renal exposure and therefore reduce renal toxicity particularly after i.v. administration.

Vorinostat is a class IV drug with low aqueous solubility and permeability. Hence, an increased bioavailability may be expected with significantly increased solubility and permeability. The dramatically enhanced aqueous solubility of vorinostat in PEG-b-PLA micelles (> 40 times vs. intrinsic solubility) can facilitate development of parenteral formulations of vorinostat and be considered as a benefit of oral micellar formulations with respect to bioavailability. The improvement of bioavailability via enhancement of aqueous solubility in nanoparticles has been seen in other drug formulations. For instance, release of genistein from nanoparticles formed with Eudragit® E100 was two times greater than that from the conventional capsules and the relative bioavailability compared with the reference suspension was 241.8% after oral administration (100 mg/kg) to fasted rats.[43,43] The reported effects of PEG-b-PLA micelles on intestinal P-glycoprotein efflux pump also may have increased the drug permeability and enhanced the oral bioavailability.[44] The micelles protect against hepatic biotransformation and first pass metabolism as indicated by lower amounts of metabolites in serum and urine, which may also account for the increased bioavailability of micellar vorinostat. The overall effects of micellar formulations on vorinostat bioavailability is likely due to a combination of these factors.

Conclusions

Micelle PEG-b-PLA formulations of vorinostat were developed that increased the water solubility by over 40-fold. PEG-b-PLA micellar systems improved the pharmacokinetics of vorinostat in rats and invoked a marked change in its biological fate characterized by statistically significant increases in serum half-life, area under curve, mean residence time, and bioavailability. These effects were more pronounced with 1:15 micelles possibly due to higher entrapment efficiency and more stable micelles *in vivo* compared to 1:10 micelles. The longer systemic residence of vorinostat in micelles was possibly due to a pronounced sustained exposure *in vivo*. Therefore, PEG-b-PLA micelles of vorinostat may be a nanoparticulate delivery system with improved disposition which could potentially lower hepatic toxicities than conventional parenteral and oral formulations. Reduced renal exposure particularly after i.v. dosing could also facilitate lower renal toxicity.

References

1. Gaucher G, Dufresne MH, Sant VP, Kang N, Maysinger D, Leroux JC. Block copolymer micelles: preparation, characterization and application in drug delivery. J Control Release. 2005; 109(1–3): 169–188. [PubMed: 16289422]

2. Kwon GS. Polymeric micelles for delivery of poorly water-soluble compounds. Crit Rev Ther Drug Carr Syst. 2003; 20(5):357–403.

3. Croy SR, Kwon GS. Polymeric micelles for drug delivery. Curr Pharm Des. 2006; 12(36):4669–4684. [PubMed: 17168771]

4. Marks PA. Discovery and development of SAHA as an anticancer agent. Oncogene. 2007; 26(9):1351–1356. [PubMed: 17322921]

5. Kavanaugh SA, White LA, Kolesar JM. Vorinostat: a novel therapy for the treatment of cutaneous T-cell lymphoma. Am J Health Syst Pharm. 2010; 67(10):793–797. [PubMed: 20479100]

6. O'Connor OA, Heaney ML, Schwartz L, Richardson S, Willim R, MacGregor-Cortelli B, Curly T, Moskowitz C, Portlock C, Horwitz S, Zelenetz AD, Frankel S, Richon V, Marks P, Kelly WK. Clinical experience with intravenous and oral formulations of the novel histone deacetylase inhibitor suberoylanilide hydroxamic acid in patients with advanced hematologic malignancies. J Clin Oncol. 2006; 24(1):166–173. [PubMed: 16330674]

7. Marks PA, Breslow R. Dimethyl sulfoxide to vorinostat: development of this histone deacetylase inhibitor as an anticancer drug. Nat Biotechnol. 2007; 25(1):84–90. [PubMed: 17211407]

8. Hrzenjak A, Moinfar F, Kremser ML, Strohmeier B, Petru E, Zatloukal K, Denk H. Histone deacetylase inhibitor vorinostat suppresses the growth of uterine sarcomas *in vitro* and *in vivo* . Mol Cancer. 2010; 9:49–59. [PubMed: 20202195]

9. Ree AH, Dueland S, Folkvord S, Hole KH, Seierstad T, Johansen M, Abrahamsen TW, Flatmark K. Vorinostat, a histone deacetylase inhibitor, combined with pelvic palliative radiotherapy for gastrointestinal carcinoma: the Pelvic Radiation and Vorinostat (PRAVO) phase 1 study. Lancet Oncol. 2010; 11(5):459–64. [PubMed: 20378407]

10. Sampson ER, Amin V, Schwarz EM, O'Keefe RJ, Rosier RN. The histone deacetylase inhibitor vorinostat selectively sensitizes fibrosarcoma cells to chemotherapy. J Orthop Res. 2011; 29(4):623–632. [PubMed: 20957741]

11. Cai YY, Yap CW, Wang Z, Ho PC, Chan SY, Ng KY, Ge ZG, Lin HS. Solubilization of vorinostat by cyclodextrins. J Clin Pharm Ther. 2010; 35(5):521–526. [PubMed: 20831676]

12. Kelly WK, Richon VM, O'Connor O, Curley T, MacGregor-Curtelli B, Tong W, Klang M, Schwartz L, Richardson S, Rosa E, Drobnjak M, Cordon-Cordo C, Chiao JH, Rifkind R, Marks PA, Scher H. Phase I clinical trial of histone deacetylase inhibitor: suberoylanilide hydroxamic acid administered intravenously. Clin Cancer Res. 2003; 9(10 Pt 1):3578–3588. [PubMed: 14506144]

13. Sandhu P, Andrews PA, Baker MP, Koeplinger KA, Soli ED, Miller T, Baillie TA. Disposition of vorinostat, a novel histone deacetylase inhibitor and anticancer agent, in preclinical species. Drug Metab Lett. 2007; 1(2):153–161. [PubMed: 19356036]

14. Venkatesh PR, Goh E, Zeng P, New LS, Xin L, Pasha MK, Sangthongpitag K, Yeo P, Kantharaj E. In vitro phase I cytochrome P450 metabolism, permeability and pharmacokinetics of SB639, a novel Histone Deacetylase Inhibitor in preclinical species. Biol Pharm Bull. 2007; 30(5):1021–1024. [PubMed: 17473456]

15. Konsoula R, Jung M. In vitro plasma stability, permeability and solubility of mercaptoacetamide histone deacetylase inhibitors. Int J Pharm. 2008; 361(1–2):19–25. [PubMed: 18562136]

16. Du L, Musson DG, Wang AQ. High turbulence liquid chromatography online extraction and tandem mass spectrometry for the simultaneous determination of suberoylanilide hydroxamic acid and its two metabolites in human serum. Rapid Commun Mass Spectrom. 2005; 19(13):1779–1787. [PubMed: 15945019]

17. Gref R, Lück M, Quellec P, Marchand M, Dellacherie E, Blunk T, Müller RH. Stealth corona-core nanoparticles surface modified by polyethylene glycol (PEG): influences of the corona (PEG chain length and surface density) and of the core composition on phagocytic uptake and plasma protein adsorption. Colloids Surf B Biointerfaces. 2000; 18(3–4):301–313. [PubMed: 10915952]

18. Bradley AJ, Murad KL, Regan KL, Scott MD. Biophysical consequences of linker chemistry and polymer size on stealth erythrocytes: size does matter. Biochim Biophys Acta. 2002; 1561(2):147–158. [PubMed: 11997115]

19. Kim K, Yu M, Zong X, Chiu J, Fang D, Seo YS, Hsiao BS, Chu B, Hadjiargyrou M. Control of degradation rate and hydrophilicity in electrospun non-woven poly(D,L-lactide) nanofiber scaffolds for biomedical applications. Biomaterials. 2003; 24(27):4977–4985. [PubMed: 14559011]

20. Zhu A, Lu P, Wu H. Immobilization of poly([var epsilon]-caprolactone)- poly(ethylene oxide)-poly([var epsilon]-caprolactone) triblock copolymer on poly(lactide-co-glycolide) surface and dual biofunctional effects. Appl Surf Sci. 2007; 253(6):3247–3253.

21. Xiao RZ, Zeng ZW, Zhou GL, Wang JJ, Li FZ, Wang M. Recent advances in PEG–PLA block copolymer nanoparticles. Int J Nanomedicine. 2010; 5:1057–1065. [PubMed: 21170353]

22. Xiao L, Xiong X, Sun X, Zhu Y, Yang H, Chen H, Lu Gan L, Xu H, Yang X. Role of cellular uptake in the reversal of multidrug resistance by PEG-b-PLA polymeric micelles. Biomaterials. 2011; 32(22):5148–5157. [PubMed: 21546083]

23. Shin HC, Alani AWG, Rao DA, Rockich NC, Kwon GS. Multi-drug loaded polymeric micelles for simultaneous delivery of poorly soluble anticancer drugs. J Control Release. 2009; 140(3):294–300. [PubMed: 19409432]

24. Shin HC, Alani AWG, Cho H, Bae Y, Kolesar JM, Kwon GS. A 3-in-1 polymeric micelle nanocontainer for poorly water-soluble drugs. Mol Pharm. 2011; 8(4):1257–1265. [PubMed: 21630670]

25. Forrest ML, Won CY, Malick AW, Kwon GS. In vitro release of the mTOR inhibitor rapamycin from poly(ethylene glycol)-b-poly(epsilon-caprolactone) micelles. J Control Release. 2006; 110(2):370–377. [PubMed: 16298448]

26. Zu Y, Wang D, Zhao X, Jiang R, Zhang Q, Zhao D, Li Y, Zu B, Sun Z. A novel preparation method for camptothecin (CPT) loaded folic acid conjugated dextran tumor-targeted nanoparticles. Int J Mol Sci. 2011; 12(7):4237–4249. [PubMed: 21845075]

27. Mohamed EA, Meshali MM, Sayre CL, Martinez SE, Remsberg CM, Borg TM, Foda AM, Davies NM. An LC/MS assay for analysis of vorinostat in rat serum and urine: application to a pre-clinical pharmacokinetic study. J Chromatograph Separat Techniq. 2012; 1(1):1000101.

28. Xiong MP, Yáñez JA, Remsberg CM, Ohgami Y, Kwon GS, Davies NM, Forrest ML. Formulation of a geldanamycin prodrug in mPEG-b-PCL micelles greatly enhances tolerability and pharmacokinetics in rats. J Control Release. 2008; 129:33–40. [PubMed: 18456363]

29. Zhan C, Gu B, Xie C, Li J, Liu Y, Lu W. Cyclic RGD conjugated poly(ethylene glycol)-co-poly(lactic acid) micelle enhances paclitaxel anti-glioblastoma effect. J Control Release. 2010; 143(1):136–142. [PubMed: 20056123]

30. Otaegui D, Rodríguez-Gascón A, Zubia A, Cossío FP, Pedraz JL. Pharmacokinetics and tissue distribution of Kendine 91, a novel histone deacetylase inhibitor, in mice. Cancer Chemother Pharmacol. 2009; 64(1):153–159. [PubMed: 19002463]

31. Fox ME, Szoka FC, Fréchet JM. Soluble polymer carriers for the treatment of cancer: the importance of molecular architecture. Acc Chem Res. 2009; 42(8):1141–1151. [PubMed: 19555070]

32. Kaminskas LM, Boyd BJ, Karellas P, Krippner GY, Lessene R, Kelly B, Porter CJH. The impact of molecular weight and PEG chain length on the systemic pharmacokinetics of PEGylated poly L-lysine dendrimers. Mol Pharmaceutics. 2008; 5(3):449–463.

33. Venkatachalam MA, Rennke HG. The structural and molecular basis of glomerular filtration. Circ Res. 1978; 43(3):337–347. [PubMed: 354819]

34. Huh KM, Lee SC, Cho YW, Lee J, Jeong JH, Park K. Hydrotropic polymer micelle system for delivery of paclitaxel. J Control Release. 2005; 101(1–3):59–68. [PubMed: 15588894]

35. Mathot F, van Beijsterveldt L, Préat V, Brewster M, Ariën A. Intestinal uptake and biodistribution of novel polymeric micelles after oral administration. J Control Release. 2006; 111(1–2):47–55. [PubMed: 16460829]

36. Gaucher G, Satturwar P, Jones MC, Furtos A, Leroux JC. Polymeric micelles for oral drug delivery. Eur J Pharm Biopharm. 2010; 76(2):147–158. [PubMed: 20600891]

37. Mathot F, des Rieux A, Ariën A, Schneider YJ, Brewster M, Préat V. Transport mechanisms of mmePEG750P(CL-co-T.MC) polymeric micelles across the intestinal barrier. J Control Release. 2007; 124(3):134–143. [PubMed: 17928087]

38. Aliabadi HM, Lavasanifar A. Polymeric micelles for drug delivery. Expert Opin Drug Deliv. 2006; 3(1):139–162. [PubMed: 16370946]

39. Dong G, Wang L, Wang CY, Yang T, Kumar MV, Dong Z. Induction of apoptosis in renal tubular cells by histone deacetylase inhibitors, a family of anticancer agents. J Pharmacol Exp Ther. 2008; 325(3):978–984. [PubMed: 18310471]

40. Rubin EH, Agrawal NG, Friedman EJ, Scott P, Mazina KE, Sun L, Du L, Ricker JL, Frankel SR, Gottesdiener KM, Wagner JA, Iwamoto M. A study to determine the effects of food and multiple dosing on the pharmacokinetics of vorinostat given orally to patients with advanced cancer. Clin Cancer Res. 2006; 12(23):7039–7045. [PubMed: 17145826]

41. Mann BS, Johnson JR, Cohen MH, Justice R, Pazdur R. FDA approval summary: vorinostat for treatment of advanced primary cutaneous T-cell lymphoma. Oncologist. 2007; 12(10):1247–1252. [PubMed: 17962618]

42. Ramalingam SS, Kummar S, Sarantopoulos J, Shibata S, LoRusso P, Yerk M, Holleran J, Lin Y, Beumer JH, Harvey RD, Ivy SP, Belani CP, Egorin MJ. Phase I study of vorinostat in patients with advanced solid tumors and hepatic dysfunction: a National Cancer Institute Organ Dysfunction Working Group study. J Clin Oncol. 2010; 28(29):4507–4512. [PubMed: 20837947]

43. Tang J, Xu N, Ji H, Liu H, Wang Z, Wu L. Eudragit nanoparticles containing genistein: formulation, development, and bioavailability assessment. Int J Nanomedicine. 2011; 6:2429–2435. [PubMed: 22072878]

44. Zhang Y, Li X, Zhou Y, Fan Y, Wang X, Huang Y, Liu Y. Cyclosporin a-loaded poly(ethylene glycol)-b-poly(d,l-lactic acid) micelles: preparation, in vitro and in vivo characterization and transport mechanism across the intestinal barrier. Mol Pharm. 2010; 7(4):1169–1182. [PubMed: 20540526]
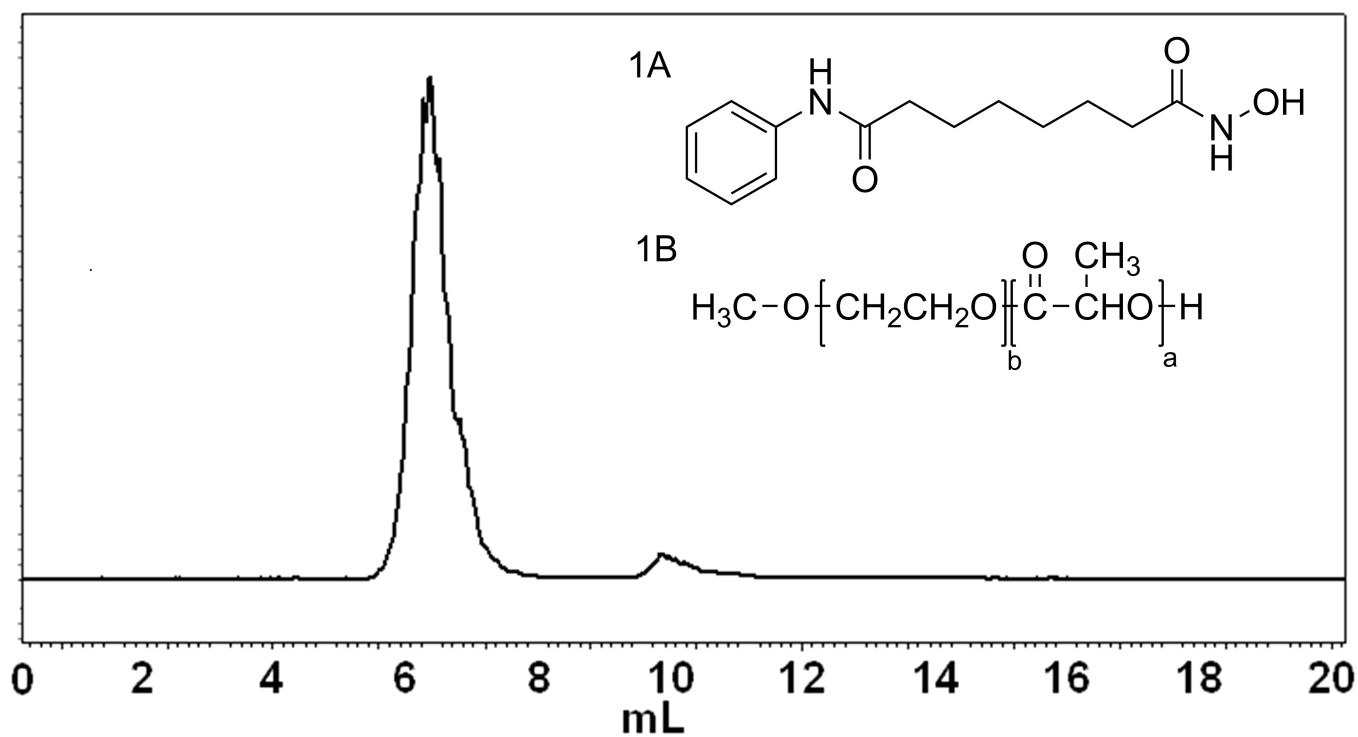
Figure 1.
SEC chromatography of PEG-b-PLA micelle in water mobile phase at 0.8 mL/min. (1A)
structure of vorinostat; (1B) structure of poly(ethylene glycol)-b-poly(lactic acid) (PEG-b-
PLA).
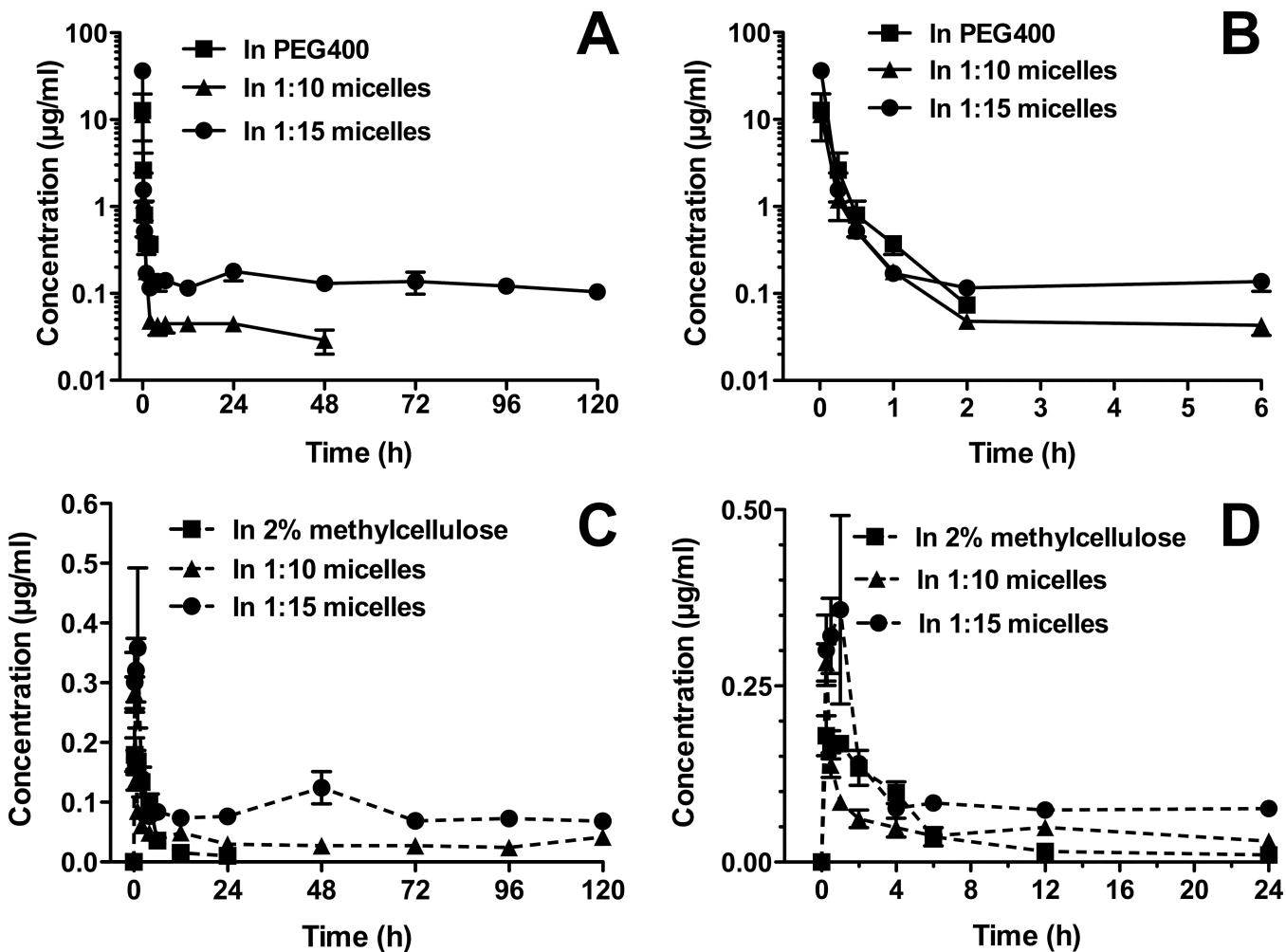
Figure 2.
Concentration-time profiles of vorinostat in rat serum after intravenous administration of vorinostat up to 120 h (A) with zoom in up to 6 h (B). Concentration-time profile of vorinostat in rat serum after oral administration of vorinostat up to 120 h (C) with zoom up to 24 h (D). The intravenous and oral doses of vorinostat for all formulations were 10 mg/kg and 50 mg/kg, respectively (mean ± SEM, $n = 5$ per group).
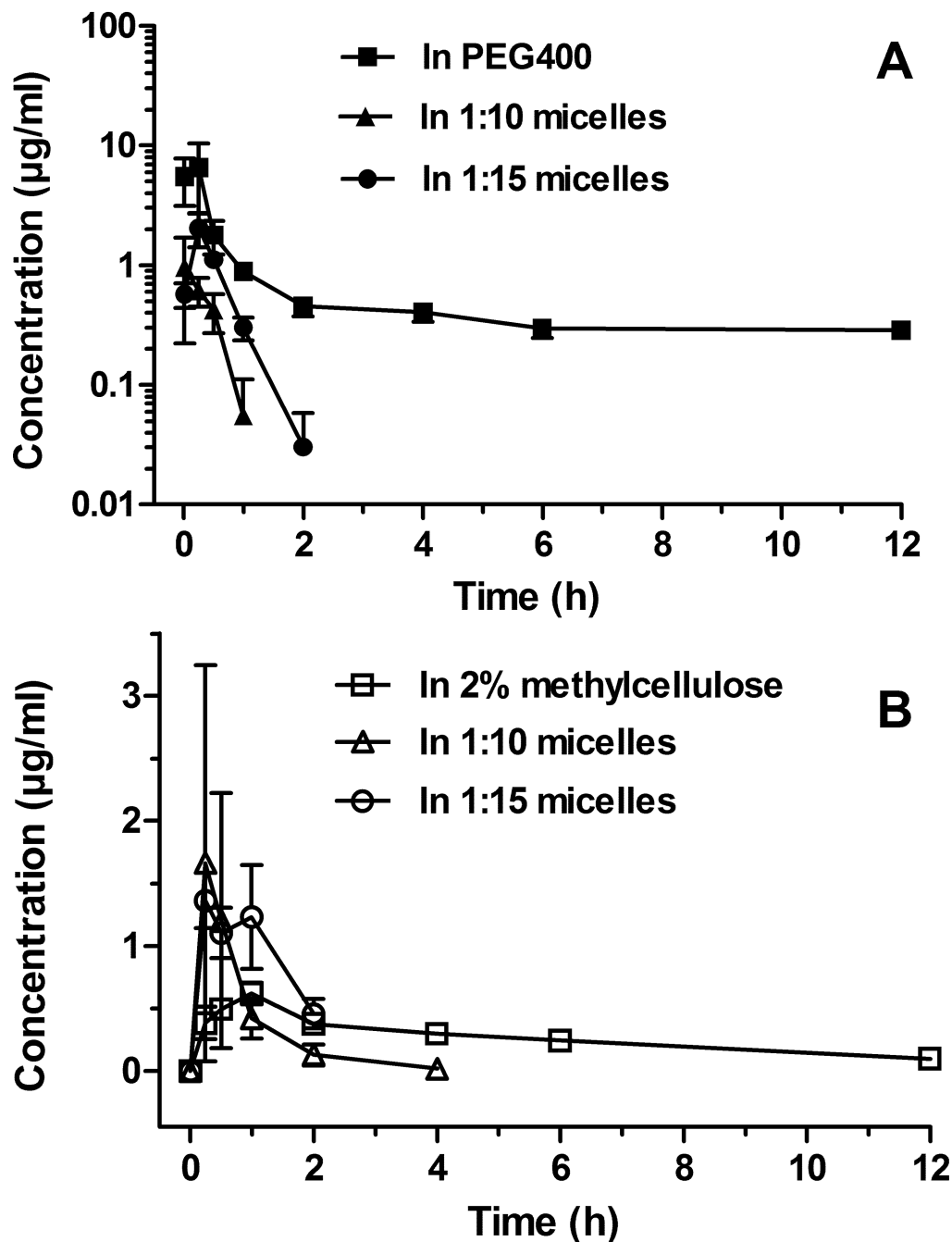
Figure 3.
Concentration-time profiles of vorinostat hydrolysis metabolite in rat serum after intravenous administration of vorinostat (A) and after oral administration of vorinostat (B). The intravenous and oral doses of vorinostat for all formulations were 10 mg/kg and 50 mg/kg, respectively (mean ± SEM, $n = 5$ per group).
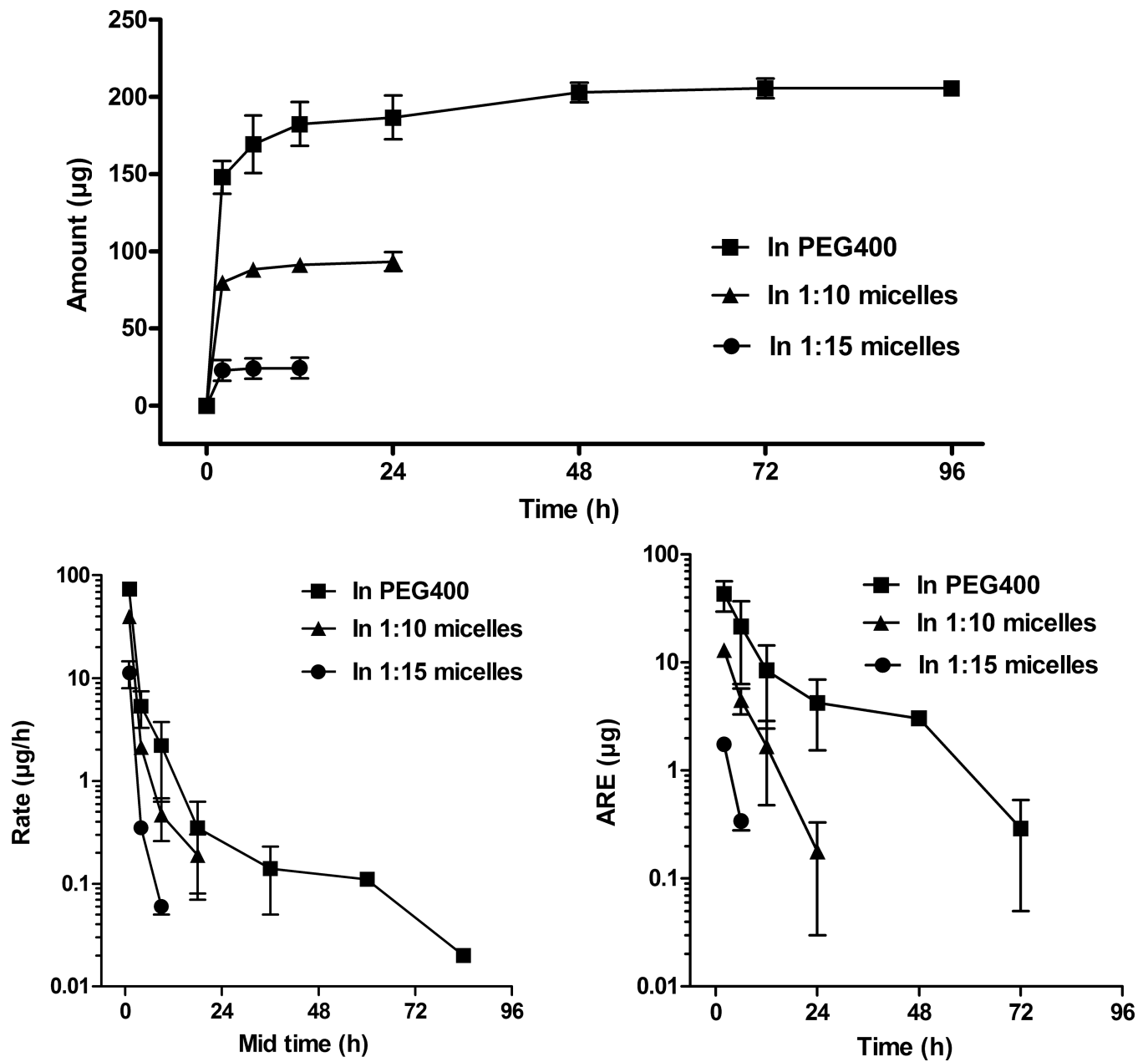
Figure 4.
(A) Total amount excreted in urine plot, (B) urinary rate plot, and (C) amount remaining to be excreted in urine (ARE) plot of vorinostat after intravenous administration of vorinostat to rats at a dose of 10 mg/kg (mean ± SEM, $n = 5$ per group).
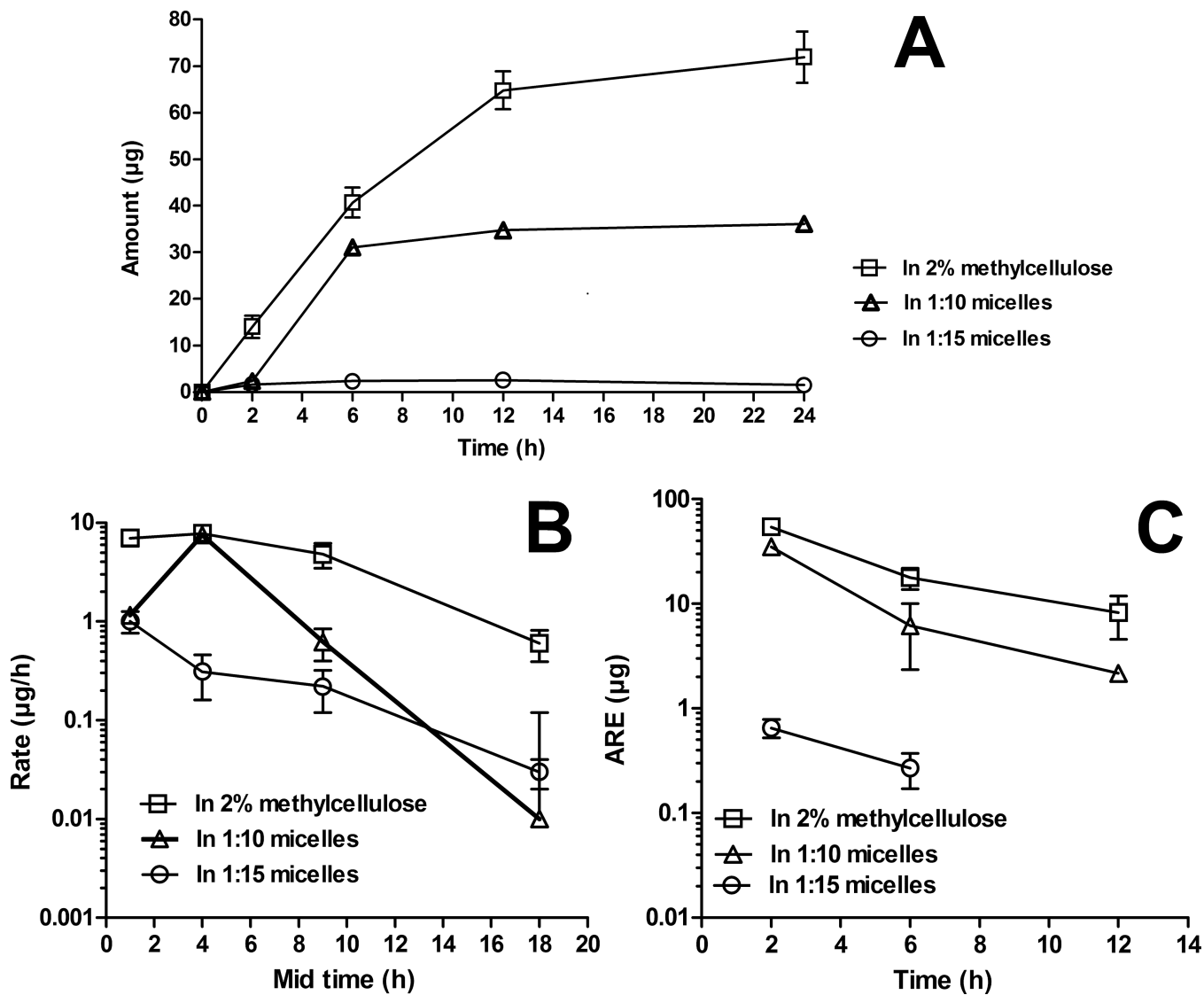
Figure 5.
(A) Total amount excreted in urine plot, (B) urinary rate plot, and (C) amount remaining to be excreted in urine (ARE) plot of vorinostat after oral administration of vorinostat to rats at a dose of 50 mg/kg (mean ± SEM, $n = 5$ per group).
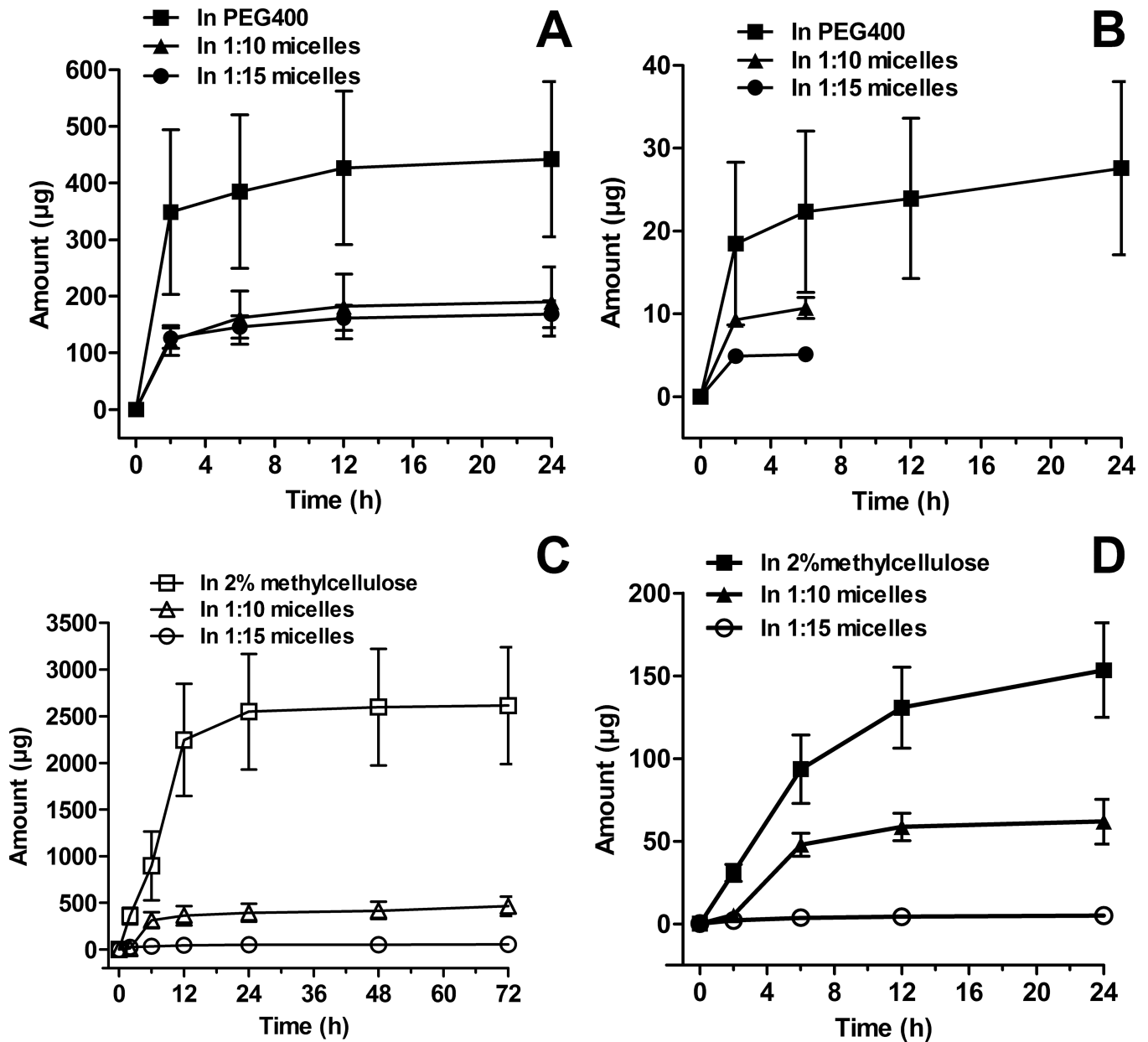
Figure 6.
Total amount excreted in urine plots of (A) the hydrolysis metabolite and (B) the glucuronide metabolite following intravenous administration of vorinostat. Total amount excreted in urine plots of (C) the hydrolysis metabolite, and (D) the glucuronide metabolite following oral administration of vorinostat. The intravenous and oral doses of vorinostat for all formulations were 10 mg/kg and 50 mg/kg, respectively (mean ± SEM, $n = 5$ per group).

Table 1

Pharmacokinetics of Vorinostat after Intravenous Administration to Rats at a Dose of 10 mg/kg (mean ± SEM, $n = 5$ per group)

Pharmacokinetic parameter	Vorinostat in PEG400 as control	Vorinostat in 1:10 PEG-b-PLA micelles	Vorinostat in 1:15 PEG-b-PLA micelles
$t_{1/2}$ (h) serum	0.61 ± 0.15	54.46 ± 18.45^{a*}	112.71 ± 19.52^{a***,b*}
F_e (%)	7.17 ± 0.96	3.17 ± 0.15^{a***}	0.83 ± 0.19 ^{a***,b*}
CL (l/h/kg)	7.64 ± 2.54	1.66 ± 0.35^{a*}	0.27 ± 0.025^{a*}
CL_{renal} (l/h/kg)	0.55 ± 0.23	0.05 ± 0.0091^{a*}	0.0022 ± 0.0007^{a*}
CL_{NR} (l/h/kg)	7.09 ± 2.32	1.61 ± 0.34^{a*}	0.26 ± 0.024^{a**}
MRT (h)	0.66 ± 0.20	70.61 ± 21.09^{a*}	153.18 ± 21.52^{a***,b**}
Vss (l/kg)	2.19 ± 0.84	16.28 ± 1.74^{a}	9.82 ± 0.68^{ab}
AUC $_{0-\infty}$ (µg.h/ml)	2.48 ± 0.98	6.77 ± 1.76	^{a***,b***} 39.01 ± 3.42

^{a}Statistically significant difference compared to vorinostat in PEG400 as control.

^{b}Statistically significant difference compared to vorinostat in 1:10 PEG-b-PLA micelles.

*$P < 0.05$,

**$P < 0.01$, and

***$P < 0.001$.

Table 2

Pharmacokinetics of Vorinostat after Oral Administration to Rats at a Dose of 50 mg/kg (mean ± SEM, $n = 5$ per group)

Pharmacokinetic parameter	Vorinostat in 2% w/v methylcellulose as control	Vorinostat in 1:10 PEG-b-PLA micelles	Vorinostat in 1:15 PEG-b-PLA micelles
$t_{1/2}$ (h) serum	3.45 ± 0.844	70.86 ± 7.106 ^{a***}	79.98 ± 13.73 ^{a***}
F_e (%)	0.53 ± 0.042	0.30 ± 0.030^{a***}	0.02 ± 0.006^{a***,b***}
CL/F (l/h/kg)	56.21 ± 4.414	8.07 ± 1.823 ^{a***}	2.99 ± 0.37^{a***}
CL_{renal}/F (l/h/kg)	0.29 ± 0.032	0.03 ± 0.007^{a***}	0.001 ± 0.0002^{a***}
CL_{NR}/F (l/h/kg)	55.92 ± 4.393	8.04 ± 1.816^{a***}	2.99 ± 0.37^{a***}
MRT (h)	5.35 ± 1.248	128.79 ± 13.489^{a***}	132.76 ± 18.66^{a***}
Vss/F (l/kg)	15.49 ± 1.22	84.13 ± 19.01^{a}	113.46 ± 13.97^{a,b}
AUC $_{0-\infty}$ (μg.h/ml)	0.91 ± 0.079	7.09 ± 0.994^{a*}	17.95 ± 2.57^{a***,b**}
F (%)	6.41 ± 0.527	58.72 ± 9.806^{a**}	98.69 ± 15.87^{a***,b*}
T_{max} (h)	0.25^{c}, 0.75^{d}	0.25^{c}, 0^{d}	0.50^{c}, 0.75^{d}
C_{max} (μg/ml)	0.198 ± 0.020	0.283 ± 0.026	0.453 ± 0.087^{a*}

[a] Statistically significant difference compared to vorinostat in 2% w/v methylcellulose suspension as control.

[b] Statistically significant difference compared to vorinostat in 1:10 PEG-b-PLA micelles.

[c,d] The median and the respective range of T_{max},

[*] $P < 0.05$,

[**] $P < 0.01$, and

[***] $P < 0.001$.